

Entanglement and transport through correlated quantum dot

Adam Rycerz

Instituut-Lorentz, Universiteit Leiden, P.O. Box 9506, NL-2300 RA Leiden, The Netherlands
Marian Smoluchowski Institute of Physics, Jagiellonian University, Reymonta 4, 30-059 Kraków, Poland
e-mail: adamr@th.if.uj.edu.pl

April 27, 2014

Abstract. We study quantum entanglement in a single-level quantum dot in the linear-response regime. The results show, that the maximal quantum value of the conductance $2e^2/h$ not always match the maximal entanglement. The pairwise entanglement between the quantum dot and the nearest atom of the lead is also analyzed by utilizing the Wootters formula for *charge* and *spin* degrees of freedom separately. The coexistence of zero concurrence and the maximal conductance is observed for low values of the dot-lead hybridization. Moreover, the pairwise concurrence vanish simultaneously for charge and spin degrees of freedom, when the Kondo resonance is present in the system.

PACS. 73.63.-b Electronic transport in nanoscale materials and structures – 03.65.Ud Entanglement and quantum nonlocality – 03.67.Mn Entanglement production, characterization, and manipulation

1 Introduction

Quantum entanglement, as one of the most intriguing features of quantum mechanics, was extensively studied during the last decade, mainly because its nonlocal connotation [1] is regarded as a valuable resource in quantum communication and information processing [2]. The question about the relation between the entanglement and quantum phase transitions [3] have been addressed recently, for either quantum spin [4,5,6] and fermionic [7,8,9] systems, in hope to shed new lights on fundamental problems of condensed matter physics. For example, it was shown for spin model [4], that the entanglement of two neighboring sites displays a sharp peak either near or at critical point where quantum phase transition undergoes. Recently, a class of systems with divergent entanglement length away from quantum critical point, since the correlation length remains finite, was identified [5]. The local entanglement was also successfully used to identify quantum phase transitions in the extended Hubbard model [9]. A separate issue concerns using the entanglement as a criterion of quantum coherence [10] when analyzing nonequilibrium dynamics of the system with spontaneous symmetry breaking [6].

Here we follow the above ideas, but focus on the physical system which undergoes the crossover behavior instead of a phase transition: a quantum dot in the Kondo regime. *Namely*, we address the question *whether there exist a relation between entanglement and conductance* for this system? Some earlier study mentioned the total entanglement of electronic degrees of freedom in the $SU(4)$ system below the Kondo temperature, without determining a qualitative measure of such an entanglement [11]. In this paper, we consider the $SU(2)$ case, and analyze two different definitions of the entanglement between quantum dot and the leads: *first* based on the von Neumann en-

tropy, and *second* utilizing the Wootters formula [12] for the formation concurrence of two-qubit system.

2 The model and its numerical solutions

We study a model of a quantum dot with a single relevant electronic level coupled to the left (L) and right (R) metallic electrodes. The Hamiltonian of the system is

$$H = H_L + V_L + H_C + V_R + H_R, \quad (1)$$

where H_C models the central region, $H_{L(R)}$ describes the left (right) lead itself, and $V_{L(R)}$ is the coupling between the lead and the central region. Namely, we have

$$H_C = \epsilon_d n_d + U n_{d\uparrow} n_{d\downarrow},$$

$$H_{L(R)} = -t \sum_{\substack{i, i+1 \in L(R) \\ \sigma=\uparrow,\downarrow}} (c_{i\sigma}^\dagger c_{i+1,\sigma} + \text{h.c.}), \quad (2)$$

$$V_{L(R)} = -V \sum_{\sigma} (c_{i_{L(R)}\sigma}^\dagger d + \text{h.c.}).$$

Here, $n_d = \sum_{\sigma} d_{\sigma}^\dagger d_{\sigma}$ is the quantum-dot charge, ϵ_d is the position of the molecular level and U is the Coulomb repulsion between two electrons. Both $H_{L(R)}$ and $V_{L(R)}$ terms have a tight-binding form, with the hopping t and the dot-lead hybridization parameter V , $c_{i\sigma}^\dagger$ ($c_{i\sigma}$) creates (destroys) an electron with spin σ on site i , the indexes $i_{L(R)}$ denotes terminal sites of the left (right) electrode. The system is depicted schematically in Fig. 1.

There are many theoretical methods in the existing literature, developed to study the electron transport in the presence

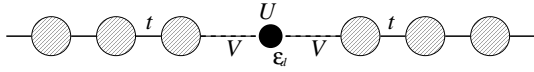


Fig. 1. The Anderson impurity model realized as a double quantum dot attached to the leads. The dot is described with the energy level ϵ_d and the Coulomb interaction U .

of interaction. In particular, the zero-temperature conductance of the quantum dot acting as an Anderson impurity were obtained within the *Bethe ansatz* approach [13]. For the more general situation, one can refer to the *Numerical Renormalization Group* [14], the nonequilibrium *Keldysh formalism* [15], and others. However, since we are interested *either* in transport properties *or* in the quantum entanglement, the most useful choice is the variational method recently proposed by Rejec and Ramšák [16, 17], in which the real-space correlation functions are obtained indirectly. For the system described by the Hamiltonian (1) the method converges to the exact solution [13], it can also be generalized for multiple quantum dots [16], for the case with a nonzero magnetic field [17], or combined with an *ab initio* wave-function readjustment [18] in the framework of EDABI method [19].

3 The quantum entanglement

For the spin $s = 1/2$ fermionic system, there are four possible local states at each site, $|\nu\rangle_j = |0\rangle_j, |\uparrow\rangle_j, |\downarrow\rangle_j, |\uparrow\downarrow\rangle_j$. The dimension of the L -site system is then 4^L and $|\nu_1, \nu_2, \dots, \nu_L\rangle = \prod_{j=1}^L |\nu_j\rangle_j$ are its natural basis vectors. Alternatively, one can label the basis vectors by specifying occupation numbers for each site and spin

$$|\nu_1 \dots \nu_L\rangle \equiv |n_{1\uparrow} \dots n_{L\uparrow}\rangle |n_{1\downarrow} \dots n_{L\downarrow}\rangle,$$

with $n_{j\sigma} = 0, 1$. The reduced density matrix for the ground state $|\Psi\rangle$ is

$$\rho_{i\sigma, j\sigma'} = \text{Tr}_{i\sigma, j\sigma'} |\Psi\rangle \langle \Psi|, \quad (3)$$

where $\text{Tr}_{i\sigma, j\sigma'}$ stands for tracing over all sites and spins except the $i\sigma$ and $j\sigma'$ -th sites.

3.1 Local entanglement entropy and conductance

We focus now on the local entanglement for the quantum dot. The reduced density matrix, defined by Eq. (3), takes the form for $i = j = d, \sigma' = \bar{\sigma}$

$$\rho_d = u_+ |0\rangle \langle 0| + w_1 |\uparrow\rangle \langle \uparrow| + w_2 |\downarrow\rangle \langle \downarrow| + u_- |\uparrow\downarrow\rangle \langle \uparrow\downarrow|, \quad (4)$$

where

$$u_+ = \langle (1 - n_{d\uparrow})(1 - n_{d\downarrow}) \rangle, \quad w_1 = \langle n_{d\uparrow}(1 - n_{d\downarrow}) \rangle,$$

$$w_2 = \langle (1 - n_{d\uparrow})n_{d\downarrow} \rangle, \quad u_- = \langle n_{d\uparrow}n_{d\downarrow} \rangle, \quad (5)$$

and the averaging is performed for the system ground state. Consequently, the corresponding von Neumann entropy is

$$E_\nu = -u_+ \log_2 u_+ - w_1 \log_2 w_1 - w_2 \log_2 w_2 - u_- \log_2 u_-. \quad (6)$$

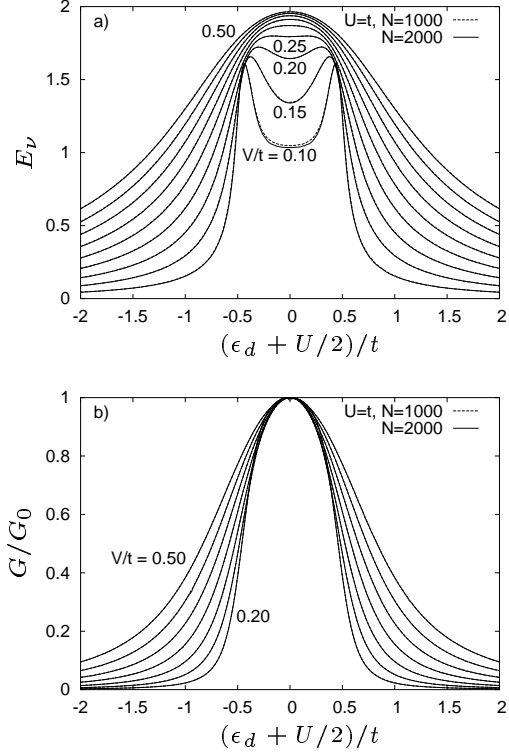


Fig. 2. The local entanglement (a) and normalized conductance (b) for the system in Fig. 1 as a function of the dot energy level ϵ_d and dot-lead hybridization V (changed in steps of $0.05t$).

In Fig. 2 we compare the the local entanglement E_ν with the conductance calculated from the Rejec–Ramšák *two-point formula* [16]

$$G = G_0 \sin^2 \frac{\pi}{2} \frac{E(\pi) - E(0)}{\Delta}, \quad (7)$$

where $G_0 = 2e^2/h$ is the conductance quantum, $\Delta = 1/N\rho(\epsilon_F)$ is the average level spacing at Fermi energy, determined by the density of states in an infinite lead $\rho(\epsilon_F)$, $E(\pi)$ and $E(0)$ are the ground-state energies of the system with *periodic* and *antiperiodic* boundary conditions, respectively. We present the numerical data for the system containing $N = 1000$ (dashed lines) and 2000 (solid lines) sites, to demonstrate the convergence of the results for both the conductance (7) and entanglement entropy (6). The latter aspect has not been analyzed numerically before. In brief, we found that the system size of the order of $N \sim 1000$ provides an excellent convergence for both the studied quantities. When calculating correlation functions (5), determining the density matrix (4), one has to choose boundary conditions which minimize the ground-state energy for a given system size N : namely, periodic for $N = 4k + 2$, and antiperiodic for $N = 4k$ [20].

Surprisingly, the maximal entanglement between a quantum dot and leads not always match the maximal conductance $G = G_0 = 2e^2/h$. For small values of the dot-lead hybridization ($V \lesssim 0.25t$ for $U = t$), where the conductance is dominated by the Kondo resonance, E_ν has a minimum at the particle-hole symmetric point $\epsilon_d = -U/2$. This observation suggest

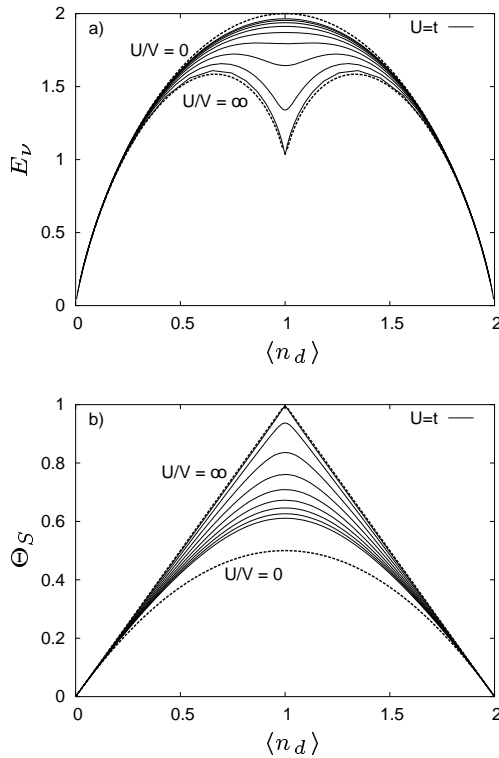


Fig. 3. The local entanglement entropy E_v (a) and spin magnitude $\Theta_S \equiv (4/3)\langle \mathbf{S}_d^2 \rangle$ (b) as a function of the dot filling $\langle n_d \rangle$ and dot–lead hybridization V . The magnitude of hybridization V goes from $0.1t$ to $0.5t$ in steps of $0.05t$. The limiting curves for $U/V = 0$ and $U/V = \infty$ are depicted with dashed lines.

an important role of the local moment formation inside the dot, which seems to determine the entanglement between the quantum dot and the leads, without observable change to the conductance. A further discussion of the relation between spin fluctuations and the entanglement is provided below.

For the better overview of the system properties we analyze then as functions of the dot filling $\langle n_d \rangle$, as displayed in *cf.* Fig. 3. The universal formula for the conductance (not shown) follows from the Luttinger theorem [21]

$$G = G_0 \sin^2(\pi \langle n_d \rangle / 2), \quad (8)$$

whereas E_v evolves gradually from the limit

$$E_v(U = 0) = -\langle n_d \rangle \log_2 \frac{\langle n_d \rangle}{2} - (2 - \langle n_d \rangle) \log_2 \left(1 - \frac{\langle n_d \rangle}{2}\right) \quad (9)$$

to

$$E_v(U = \infty) = -(1 - \langle n_d \rangle) \log_2 (1 - \langle n_d \rangle) - \langle n_d \rangle \log_2 \frac{\langle n_d \rangle}{2}, \quad (10)$$

as presented in Fig. 3a. Therefore, in the strong coupling limit E_v has two maxima at $\langle n_d \rangle = 2/3$ and $4/3$, instead of a single

for $\langle n_d \rangle = 1$, present in the noninteracting case. One can also observe, that the entanglement behavior near the particle–hole symmetric point $\langle n_d \rangle = 1$ is determined by the magnitude of spin fluctuations, presented in Fig. 3b. As a measure of such fluctuations, we define a parameter

$$\Theta_S \equiv \frac{4}{3}\langle \mathbf{S}_d^2 \rangle = \langle n_d \rangle - 2\langle n_{d\uparrow}n_{d\downarrow} \rangle,$$

which obeys the inequality

$$\langle n_d \rangle \left(1 - \frac{\langle n_d \rangle}{2}\right) \leq \Theta_S \leq 1 - |1 - \langle n_d \rangle|, \quad (11)$$

where the lower and the upper limit refers to the $U = 0$ and $U = \infty$ case, respectively.

The correspondence between the inequality (11) and the limits defined by Eqs. (9) and (10) become straightforward when expressing the coefficients of the density matrix (4) as functions of $\langle n_d \rangle$ and Θ_S , what leads to the entanglement entropy

$$E_v = -\left(\frac{2 - \langle n_d \rangle - \Theta_S}{2}\right) \log_2 \left(\frac{2 - \langle n_d \rangle - \Theta_S}{2}\right) - \left(\frac{\langle n_d \rangle - \Theta_S}{2}\right) \log_2 \left(\frac{\langle n_d \rangle - \Theta_S}{2}\right) - \Theta_S \log_2 \frac{\Theta_S}{2}. \quad (12)$$

Eq. (12) with the limits given by (11) relates the entanglement between the quantum dot and the leads to the local moment formation inside the dot. It also express the entanglement entropy in terms of measurable quantities: the dot occupation $\langle n_d \rangle$ and the spin–square magnitude $\langle \mathbf{S}_d^2 \rangle$. In contrast, the spin fluctuations are absent in Eq. (8) for the conductance, which is fully determined by the dot filling $\langle n_d \rangle$.

3.2 The fermionic concurrence

The reduced density matrix for the pair of electrons with equal spins (say $\sigma = \uparrow$), one localized on a quantum dot and other on a nearest lead atom ($i = d, j = j_{L(R)}$), has the form

$$\rho_{i\uparrow,j\uparrow} = \begin{pmatrix} u_+^c & 0 & 0 & 0 \\ 0 & w_1^c & z^c & 0 \\ 0 & (z^*)^c & w_2^c & 0 \\ 0 & 0 & 0 & u_-^c \end{pmatrix}, \quad (13)$$

where

$$\begin{aligned} u_+^c &= \langle (1 - n_{i\uparrow})(1 - n_{j\uparrow}) \rangle, & u_-^c &= \langle n_{i\uparrow}n_{j\uparrow} \rangle, \\ w_1^c &= \langle n_{i\uparrow}(1 - n_{j\uparrow}) \rangle, & w_2^c &= \langle (1 - n_{i\uparrow})n_{j\uparrow} \rangle, \\ z^c &= \langle c_{j\uparrow}^\dagger c_{i\uparrow} \rangle. \end{aligned} \quad (14)$$

The upper index c stands to denote, that the density matrix (13) refers to the *charge* degrees of freedom, since the *spin* direction is arbitrarily chosen for both particles.

We use now the *concurrence* \mathcal{C} as a measure of the entanglement for such a two–qubit system. The closed–form expression, first derived by Wootters [12], reads

$$\mathcal{C} = \max \left\{ 0, \sqrt{\lambda_1} - \sqrt{\lambda_2} - \sqrt{\lambda_3} - \sqrt{\lambda_4} \right\}. \quad (15)$$

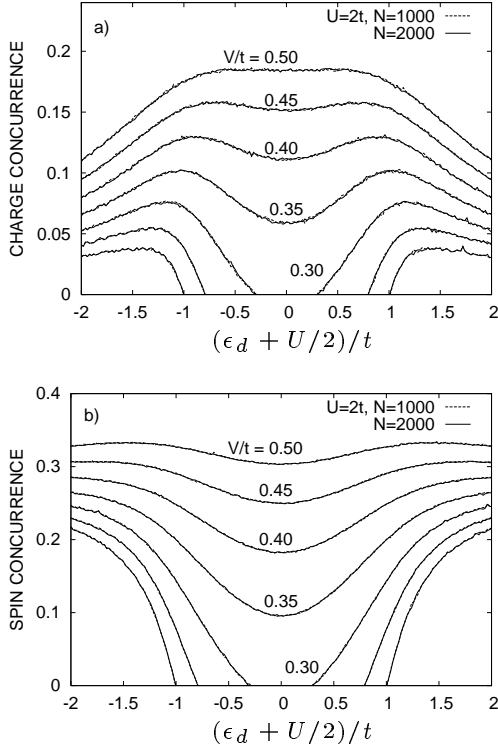


Fig. 4. The charge (a) and spin (b) pairwise concurrence for the system containing one qubit localized on quantum dot and the second on the nearest atom of the lead.

The λ_i 's are the eigenvalues of the matrix product $\rho \cdot \bar{\rho}$, where

$$\bar{\rho} = (\sigma_i^y \otimes \sigma_j^y) \rho^* (\sigma_i^y \otimes \sigma_j^y), \quad (16)$$

in the order $\lambda_1 \geq \lambda_2 \geq \lambda_3 \geq \lambda_4$. Since there exists a monotonous relation between the concurrence and the entanglement entropy of formation $E_f = -x \log_2 x - (1-x) \log_2 (1-x)$, where $x = 1/2 + \sqrt{1 - \mathcal{C}^2}/2$ [12], it is widely used of instead E_f in the literature.

For the density matrix $\rho_{i\uparrow,j\uparrow}$ given by Eq. (13) the corresponding concurrence can be calculated from Eq. (15) as

$$\mathcal{C}_{i\uparrow,j\uparrow} = 2 \max \left\{ 0, \left| \langle c_{i\uparrow}^\dagger c_{j\uparrow} \rangle \right| - \sqrt{\langle n_{i\uparrow} n_{j\uparrow} \rangle (1 - \langle n_{i\uparrow} \rangle - \langle n_{j\uparrow} \rangle + \langle n_{i\uparrow} n_{j\uparrow} \rangle)} \right\}. \quad (17)$$

Hereinafter, we call $\mathcal{C}_{i\uparrow,j\uparrow}$ a *charge concurrence*, since it is related to the charge degrees of freedom.

Alternatively, one can consider the full two-site density matrix ρ_{ij} (with $i = d$, and $j = j_{L(R)}$ again) and project out all the states except from these corresponding to $n_i = n_j = 1$. The resultant 4×4 density matrix

$$\rho_{s_i, s_j} = \frac{1}{\text{Tr} \tilde{\rho}_{s_i, s_j}} \tilde{\rho}_{s_i, s_j} \quad (18)$$

describes the entanglement accessible by spin manipulation with a particle-conservation constrain [22]. The matrix $\tilde{\rho}_{s_i, s_j}$ has a

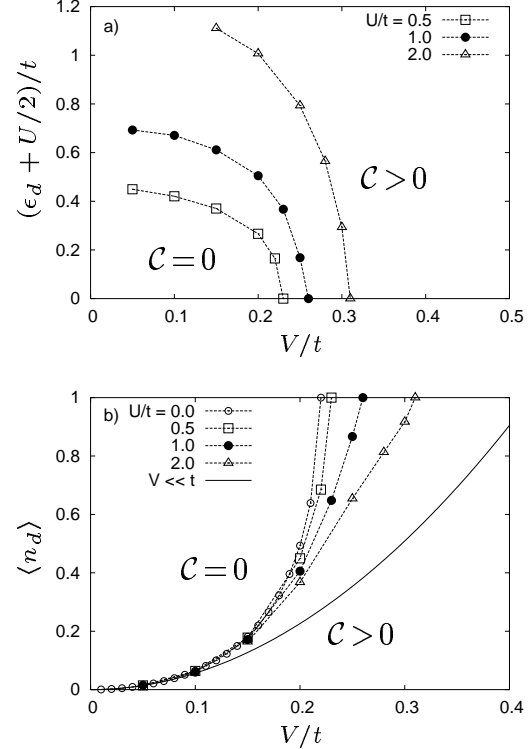


Fig. 5. The values of dot energy level ϵ_d (a) and average occupation $\langle n_d \rangle$ (b) corresponding to zero concurrence, as a function of hybridization V and Coulomb interaction U (specified for each dataset). The perturbative limit $V \ll t$ is also shown.

general structure of $\rho_{i\uparrow,j\uparrow}$ given by Eq. (13), with the elements (14) replaced by

$$\begin{aligned} u_+^s &= \langle n_{i\uparrow} (1 - n_{i\downarrow}) n_{j\uparrow} (1 - n_{j\downarrow}) \rangle, \\ u_-^s &= \langle (1 - n_{i\uparrow}) n_{i\downarrow} (1 - n_{j\uparrow}) n_{j\downarrow} \rangle, \\ w_1^s &= \langle n_{i\uparrow} (1 - n_{i\downarrow}) (1 - n_{j\uparrow}) n_{j\downarrow} \rangle, \\ w_2^s &= \langle (1 - n_{i\uparrow}) n_{i\downarrow} n_{j\uparrow} (1 - n_{j\downarrow}) \rangle, \\ z^s &= \langle S_j^+ S_i^- \rangle = \langle c_{j\uparrow}^\dagger c_{j\downarrow} c_{i\downarrow}^\dagger c_{i\uparrow} \rangle. \end{aligned} \quad (19)$$

The label s indicates that we are working know with the *spin* degrees of freedom, as charges of the i and j sites are chosen. The concurrence, obtained by applying the definition (15) to the density matrix (18), is called a *spin concurrence*.

The charge and spin concurrence is shown in Fig. 4 as a function of the dot energy level ϵ_d . Again, we observe an excellent convergence of both the studied quantities for the system size of the order of $N \sim 1000$. Although the charge and spin concurrence are, in principle, two different physical quantities, they reach the limit $\mathcal{C} = 0$ simultaneously for all the analyzed values of V and U . Therefore, we can conclude that below the critical value of the hybridization $V < V_c(U)$ and in the Kondo regime, the qubit localized on the quantum dot is not entangled with other placed on the top of the lead for *neither* charge *nor* spin degrees of freedom. The values of ϵ_d

and $\langle n_d \rangle$, corresponding to $\mathcal{C} = 0$ are depicted in Fig. 5. Probably, the most interesting feature of these results is the universal (interaction independent) behavior of the maximal dot filling $\langle n_d \rangle = \langle n_d \rangle_{\max}$, for which the entanglement $\mathcal{C} \geq 0$, with $V/t \rightarrow 0$ (cf. Fig. 5b). This observation can be rationalized by using Eq. (17) and putting $\mathcal{C}_{i\uparrow,j\uparrow} = 0$. Then, in the perturbative limit $V \ll t$, we obtain

$$\langle n_d \rangle_{\max} \approx 2^{3/2} |\langle c_i^\dagger c_j \rangle| \approx 2^{5/2} (V/t)^2,$$

up to the quadratic terms. The agreement with the numerical data is perfect for $V/t \leq 0.1$.

4 Summary

We analyzed the local entanglement between the quantum dot and the leads as a function of the dot energy level ϵ_d , the dot-lead hybridization V and the intra-dot Coulomb repulsion U . The measure of this entanglement, the von Neumann entropy E_ν , evolves gradually from the *weak-coupling* limit, in which the maximal E_ν match the maximal quantum value of the conductance $G = G_0 = 2e^2/h$, to the *strong-coupling* situation, where maximal G corresponds to the local minimum of E_ν . This behavior was explained in terms of local moment formation inside the dot, which took place when the charge transport is dominated by the Kondo effect.

Finally, we defined the pairwise concurrence, measuring the entanglement between a pair of qubits: one localized on the dot second on the nearest atom of the lead, for *charge* and *spin* degrees of freedom separately. Both quantities vanish simultaneously in the Kondo-resonance range, where the weakly-entangled system show the maximal conductance. The universal dependence of the maximal dot filling, above which the concurrence vanish, $\langle n_d \rangle_{\max} \approx 2^{5/2} (V/t)^2$ for $V/t \ll 1$, was also identified.

Acknowledgment

The author thanks C. W. J. Beenakker for many discussions. Remarks by M. A. Martin-Delgado and D. Sanchez are appreciated. The work was supported by the Polish Science Foundation (FNP) Foreign Postdoc Fellowship, and by Polish Ministry of Education and Science, Grant No. 1 P03B 001 29.

References

1. A. Einstein, B. Podolski, and N. Rosen, *Phys. Rev.* **47**, 777 (1935).
2. See review by C. H. Bennet and D. P. Divincenzo, *Nature* **404**, 247 (2000); M. A. Nielsen and I. L. Chuang, *Quantum Computation and Quantum Information* (Cambridge, 2000).
3. S. Sachdev, *Quantum Phase Transitions* (Cambridge University Press, Cambridge, 2000).
4. A. Osterloh *et al.*, *Nature* **416**, 608 (2002); T. J. Osborne and M. A. Nielsen, *Phys. Rev. A* **66**, 032110 (2002); V. Subrahmanyam, *ibid.* **69**, 022311 (2004).
5. F. Verstraete, M. A. Martin-Delgado, J. I. Cirac, *Phys. Rev. Lett.* **92**, 087201 (2004); M. Popp *et al.*, *quant-ph/0411123*, unpublished.
6. J. van Wenzel, J. van den Brink, J. Zaanen, *Phys. Rev. Lett.* **94**, 230401 (2005).
7. J. Schliemann, D. Loss, A. H. MacDonald, *Phys. Rev. B* **63**, 085311 (2001); J. Schliemann *et al.*, *Phys. Rev. A* **64**, 022303 (2001).
8. P. Zanardi, *Phys. Rev. A* **65**, 042101 (2002); P. Zanardi, X. Wang, *J. Phys. A* **35**, 7947 (2002).
9. S.-J. Gu *et al.*, *Phys. Rev. Lett.* **93**, 086402 (2004).
10. A. O. Caldeira and A. J. Leggett, *Phys. Rev. Lett.* **46**, 211 (1981); I. L. Chuang *et al.*, *Science* **270**, 1633 (1995).
11. M.-S. Choi, R. López, R. Aguado, *Phys. Rev. Lett.* **95**, 067204 (2005); R. López *et al.*, *Phys. Rev. B* **71**, 115312 (2005).
12. W. K. Wootters, *Phys. Rev. Lett.* **80**, 2245 (1998); S. Hill, W. K. Wootters, *Phys. Rev. Lett.* **78**, 5022 (1997).
13. P. B. Wiegman, A. M. Tsvelick, *Pis'ma ZETF* **35**, 100 (1982); *J. Phys. C* **16**, 2281 (1983).
14. W. Hofstetter, J. König, and H. Schoeller, *Phys. Rev. Lett.* **87**, 156803 (2001).
15. Y. Meir, N. S. Wingreen, *Phys. Rev. Lett.* **68**, 2512 (1992).
16. T. Rejec, A. Ramšak, *Phys. Rev. B* **68**, 035342 (2003).
17. T. Rejec, A. Ramšak, *Phys. Rev. B* **68**, 033306 (2003).
18. A. Rycerz, J. Spałek, *cond-mat/0604237*, *Physica B*, *in press*.
19. A. Rycerz, J. Spałek, *Eur. Phys. J. B* **40**, 153 (2004); *Phys. Rev. B* **63**, 073101 (2001); *ibid.* **65**, 035110 (2002).
20. E. H. Lieb, *Phys. Rev. Lett.* **73**, 2158 (1994); F. Nakano, *J. Phys. A* **33**, 5429 (2000); *ibid.* **37**, 3979 (2004). For a discussion of boundary condition role in even/odd effect for correlated nanosystems see: A. Rycerz, J. Spałek, *phys. stat. sol. (b)* **243**, 183 (2006).
21. A. C. Hewson, *The Kondo Problem to Heavy Fermions* (Cambridge University Press, 1997).
22. See, e.g. C. W. J. Beenakker, *cond-mat/0508488*, to be published in *Quantum Computers, Algorithms and Chaos*, Int. School of Phys. “Enrico Fermi”, vol. 162, and references therein.